

## What Makes a Natural Clay Antibacterial?

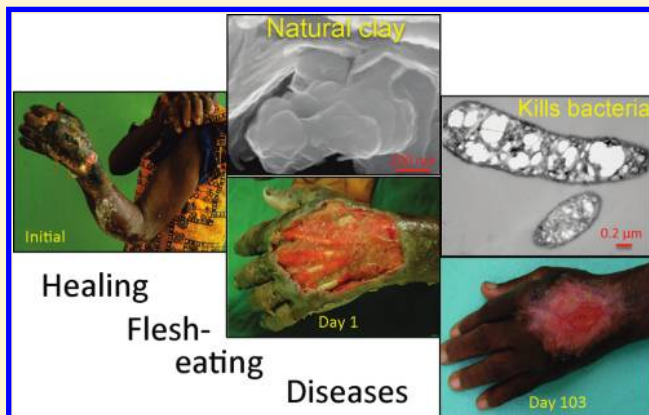
Lynda B. Williams,<sup>†,\*</sup> David W. Metge,<sup>‡</sup> Dennis D. Eberl,<sup>‡</sup> Ronald W. Harvey,<sup>‡</sup> Amanda G. Turner,<sup>†</sup> Panjai Prapaipong,<sup>†</sup> and Amisha T. Poret-Peterson<sup>†</sup>

<sup>†</sup>School of Earth & Space Exploration, Arizona State University, Tempe, Arizona 85287, United States

<sup>‡</sup>U.S. Geological Survey, 3215 Marine St., Suite E127, Boulder, Colorado 80303, United States

**ABSTRACT:** Natural clays have been used in ancient and modern medicine, but the mechanism(s) that make certain clays lethal against bacterial pathogens has not been identified. We have compared the depositional environments, mineralogies, and chemistries of clays that exhibit antibacterial effects on a broad spectrum of human pathogens including antibiotic resistant strains. Natural antibacterial clays contain nanoscale (<200 nm), illite-smectite and reduced iron phases. The role of clay minerals in the bactericidal process is to buffer the aqueous pH and oxidation state to conditions that promote Fe<sup>2+</sup> solubility.

Chemical analyses of *E. coli* killed by aqueous leachates of an antibacterial clay show that intracellular concentrations of Fe and P are elevated relative to controls. Phosphorus uptake by the cells supports a regulatory role of polyphosphate or phospholipids in controlling Fe<sup>2+</sup>. Fenton reaction products can degrade critical cell components, but we deduce that extracellular processes do not cause cell death. Rather, Fe<sup>2+</sup> overwhelms outer membrane regulatory proteins and is oxidized when it enters the cell, precipitating Fe<sup>3+</sup> and producing lethal hydroxyl radicals.



### INTRODUCTION

Overuse of antibiotics in healthcare is a major concern because of the consequential proliferation of antimicrobial resistance. Our studies of natural antibacterial minerals were initiated to investigate alternative antimicrobial mechanisms. Indigenous people worldwide have used clays for healing throughout history. French green clay poultices were documented for healing Buruli ulcer,<sup>1</sup> a necrotizing fasciitis caused by *Mycobacterium ulcerans*. However, only one of the French clays used for healing proved to be antibacterial.<sup>2</sup> Other sources of French green clay increased bacteria growth relative to controls.<sup>3</sup> Continued testing of clays worldwide has revealed only a few deposits that are antibacterial. Each deposit is mineralogically different, but they are all from hydrothermally altered volcanoclastic environments; either altered pyroclastic material or bentonite (volcanic ash).

This paper reports the geochemical characteristics of the most effective antibacterial clay we have identified; supplied by Oregon Mineral Technologies (OMT) Grants Pass, Oregon. The clay source is an open pit mine in hydrothermally altered, pyroclastic material in the Cascade Mountains. It was shown to completely eliminate *Escherichia coli*, *Staphylococcus aureus*, *Pseudomonas aeruginosa*, *Salmonella typhimurium*, and antibiotic resistant extended-spectrum beta lactamase (ESBL) *E. coli* and methicillin resistant *S. aureus* (MRSA) within 24 h.<sup>4</sup>

A variety of physical and/or chemical processes can make clays antibacterial. Physical bactericide can occur by surface attraction

between clay minerals and bacteria, which can hamper passive and active uptake of essential nutrients, disrupt cell envelopes or impair efflux of metabolites.<sup>5</sup> The natural antibacterial clays we have studied do not kill by physical associations between the clay and bacterial cells.<sup>6</sup> The OMT clay shows no zone of inhibition when applied dry to bacterial colonies in vitro; however, the clays are antibacterial when hydrated. When an aqueous suspension of OMT clay (50 mg/mL water) was placed in dialysis tubing (25 000 MDCO) and submerged into a beaker of *E. coli* suspended in sterile Tryptic soy broth, the bacteria died over 24 h.<sup>7</sup> Comparisons have been made between aqueous leachates of the OMT clay incubated with *E. coli* in nutrient broth and without nutrient broth<sup>2</sup> to eliminate chemical speciation influenced by the broth chemistry. *E. coli* are completely killed by OMT leachates rapidly (Figure 1), compared to controls in distilled–deionized (DDI) water. Cell death occurs by exchange of soluble clay constituents toxic to the bacteria.

Other clays, for example, allophane and imogolite, have been made antibacterial by chemical sorption of known bactericidal elements (Ag, Cu, Co, Zn) onto certain crystallographic sites of the mineral surfaces.<sup>8–10</sup> Nanoparticulate metal oxides and

**Received:** December 5, 2010

**Accepted:** March 3, 2011

**Revised:** February 27, 2011

**Published:** March 17, 2011

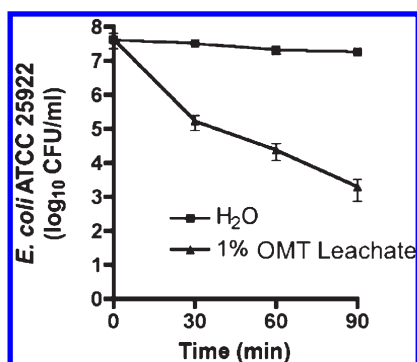


**Figure 1.** Kill curve for a 10 mg/mL (1%) suspension of the OMT clay in DDI water. The top line shows that the control bacterial population was not significantly affected by the lack of nutrients over this time period.

ceramics can also be antibacterial,<sup>11</sup> releasing soluble toxic compounds in proportion to their high specific surface area.<sup>12,13</sup> Consequently, our objective is to document what soluble elements *E. coli* assimilate from the natural antibacterial OMT clay.

## EXPERIMENTAL METHODS

Aqueous leachates were prepared using sterilized clay and water (50 mg/mL). The mixture was ultrasonified (Branson Sonifier 450) then shaken 24 h to equilibrate. The suspension of minerals in water was centrifuged (20 000 rpm; 67 000g) 1 h to remove solids<sup>14</sup> and the solution was decanted.

*E. coli* (JM109) was grown to log phase and a cell density of  $\sim 10^9$  cfu/mL in Luria Broth (LB). The cell population produced  $\sim 30$  mg of cells (dry wt.) per experiment and each experiment was repeated in triplicate. *E. coli* was incubated in 1:1 volume ratio with clay leachate. All cultures were grown at 37 °C in a shaker-incubator for 24 h. Bacterial growth was evaluated after incubation, by standard plate counts. Bacteria (live or dead) from experiments were centrifuged at 7000 rpm for 5 min to pellet. Bacterial cells were then rinsed with DDI water (25 mL) in triplicate. Finally, one aliquot was rinsed in 25 mL of 50 mM EDTA:100 mM oxalic acid with 0.85% NaCl (pH adjusted to 6.95 with NaOH). This oxalate-EDTA solution removes metals from the exterior cell envelope<sup>15</sup> without causing cell lysis.<sup>16</sup> Test tubes containing bacteria were dried at room temperature, ground, and accurately weighed. Twelve milliliters of 10% nitric acid (Omnitrace Ultra, EMD chemicals) was used to digest cells, and then diluted to 40 mL.

Leachates, whole cells, and cells with exterior metals removed, were analyzed for elemental compositions with a Thermo Fisher Element 2 single-collector, double-focusing magnetic sector inductively coupled plasma mass spectrometer (ICP-MS) in low-, medium-, and high-resolution modes, depending on spectral interferences. The samples, blanks, and standards were acidified with nitric acid and spiked with 1 ppb indium solution to correct for instrumental response affected by solution matrix. Analyses of river water standard reference materials NIST 1640, NIST 1643e, and NRC SLRS4 determined analytical accuracy and precision. The measurement uncertainties were <5% ( $1\sigma$ ). Major anion concentrations were measured by ion chromatography using a Dionex DX 600 Dual IC System with IonPac AS11-HC column.

**Table 1.** Mineralogy of Two Antibacterial Clays (ARG and OMT) Compared to Non-Antibacterial Clay (NAB), by Quantitative X-ray Diffraction<sup>17</sup> Using CuK $\alpha$  Radiation<sup>a</sup>

ARG		OMT		NAB	
mineral	wt%	mineral	wt%	mineral	wt%
Clay Minerals		Clay Minerals		Clay Minerals	
1Md Illite (+ smectite)	30	Illite-smectite (R1)	49.6	kaolins	2.4
Fe-smectite	33	chlorite	3.1	Ca smectite	3.0
1 M Illite (R > 2)	13			Fe-smectite	8.3
mica (2M <sub>1</sub> )	3.3			biotite (1M)	13.6
				mica (2M <sub>1</sub> )	4.1
				chlorite	6.0
Non-Clays		Non-Clays		Non-Clays	
quartz	2.0	quartz	38.3	quartz	6.2
calcite	4.4	amphibole	0.5	plagioclase	43.9
microcline	3.4	pyrite	8.2	Fe-amphibole	3.8
orthoclase	2.9	jarosite	0.2	pyrite	0.7
albite	1.6	gypsum	0.9	gypsum	2.0
				apatite	0.5
<b>total nonclays</b>	<b>14</b>	<b>total nonclays</b>	<b>48.1</b>	actinolite	2.7
				calcite	0.8

<sup>a</sup>Notation: R = Reichweite (ordering); M = monoclinic; Md = monoclinic disordered.

## RESULTS

Each antibacterial clay deposit is mineralogically different (Table 1) but they have in common the presence of expandable clay minerals (smectite) and Fe-rich phases (e.g., Fe-smectite, biotite, jarosite, pyrite, magnetite, hematite, goethite, amphibole). The presence of pyrite in some samples may be important for bactericidal action,<sup>18</sup> but not all antibacterial clays contain pyrite. The average crystal diameter of the antibacterial clays (<200 nm) is an order of magnitude smaller than standard clay reference materials.<sup>19</sup> The nanominerals in these deposits may enhance solubility of toxic elements.<sup>20</sup> Additionally, the smectite may sequester toxic ions in the interlayer sites, which could be released upon rehydration in a clay poultice.

Table 2 presents the chemistry of aqueous leachates from the OMT clay compared to the French antibacterial clay (ARG)<sup>3</sup> and a nonantibacterial clay (NAB)<sup>21</sup> used medicinally. The elemental concentrations are all below minimum inhibitory concentrations (MIC) published for *E. coli* at circum-neutral pH.<sup>22–24</sup> However, under the pH, oxidation state and aqueous speciation created within a clay poultice, the MIC may be quite different due to stabilization of different soluble species.

*E. coli* (JM109) was used as a model species to evaluate mass transfer from the clay to bacteria. Incubation of the antibacterial OMT leachate 1:1 with a population of  $10^9$  cfu/mL *E. coli* grown in LB to log phase, showed no surviving bacteria in three independent experiments, compared to nonantibacterial (NAB) clay leachate and control (*E. coli* in LB without leachate). The control group produced on average  $7.9 \pm 0.4 \times 10^9$  cfu/mL, and the NAB clay leachate produced  $9.0 \pm 0.8 \times 10^9$  cfu/mL. Elements taken up by the OMT clay-amended *E. coli* suspensions were analyzed using direct injection ICP-MS<sup>25</sup> (Table 3). Only elements showing significant differences in concentration from the controls are presented. Whole cells were rinsed in triplicate

**Table 2. Chemical Analyses of Aqueous Clay Leachates, (A) ICP-MS Analyses of the Antibacterial ARG Clay<sup>3</sup>, the OMT (This Study) and NAB Clay Leachate<sup>21</sup>, (B) Ion Chromatography Analysis of Anions in the OMT Leachate<sup>a</sup>**

(A)	ARG	ARG	OMT	OMT	NAB	NAB
element	$\mu\text{g/L}$	$\mu\text{M}$	$\mu\text{g/L}$	$\mu\text{M}$	$\mu\text{g/L}$	$\mu\text{M}$
Mg	620	26	20900	860	93 000	3826
Al	5040	187	23900	886	13 400	497
Si	7400	264	1430	51	na	na
P	446	14	96	3	7.3	0.24
K	7700	197	210	5	na	na
Ca	3500	87	$2 \times 10^5$	4341	88 000	2196
V	21.5	0.42	3.3	0.06	1.1	0.02
Cr	1.3	0.03	16	0.30	na	na
Mn	55	1.0	5170	94	4300	78
Fe	280	5.0	51 600	924	10 500	188
Co	0.1	0.002	204	3	102	1.73
Ni	4.4	0.07	169	3	60	1.02
Cu	2.7	0.04	225	4	63	0.99
Zn	5.0	0.08	1090	17	66	1.01
As	260	3.47	1.1	0.01	0.4	0.01
Se	1.5	0.02	2.3	0.03	0.3	0.00
Rb	18	0.21	0.18	0.00	7.1	0.08
Sr	58	0.66	338	4	186	2.12
Ba	31	0.23	5.5	0.04	11	0.08
Pb	0.26	0.001	0.02	0.0001	0.08	0.0004
pH	10		4		8	

(B)	OMT leachate anions					
	$\text{Cl}^-$	$\text{NO}_2^-$	$\text{NO}_3^-$	$\text{Br}^-$	$\text{SO}_4^{2-}$	$\text{PO}_4^{3-}$
ppm	0.88	nd	nd	nd	2065	6.6
%rsd	1.4				0.06	4.9

<sup>a</sup> na = not analyzed; nd = none detected; %rsd = % relative std. dev. of three analyses.

with filter-sterilized, distilled–deionized (DDI) water before elemental measurements. Intracellular elemental abundances were determined on oxalate-EDTA treated samples, which removes extracellular metals, particularly Fe.<sup>15</sup>

High-resolution scanning electron microscope (SEM) images of the OMT clay (Figure 2) show (a) the dominance of submicrometer crystals; (b) the clay matrix encompassing submicrometer spherical Fe–S particles; and (c) coexistence of a lath-shaped mineral rich in Ca, Al, S, and O (sulfate). Different batches of OMT contain up to 3wt.% gypsum and/or jarosite. Coexistence of gypsum and pyrite in the natural clay places the equilibrium chemical stability on the equal activity line for S–SO<sub>4</sub>.<sup>26</sup>

Important energy-requiring processes for nutrient uptake and metabolism, motility, and cell division occur at the cell membrane. Transmission electron microscope (TEM) imaging of *E. coli* treated with the OMT leachate (Figure 3) shows initial development of “hairy” vesicles on the cell membrane in response to acidic conditions.<sup>27</sup> Black, electron-opaque, particles are initially evenly distributed on the cell walls. However, after 6 h of incubation, the black particles are concentrated at polar ends of the cells, indicating that the cells are metabolically active, as bacteria regulate uptake of metals through polar attractions.<sup>28</sup>

**Table 3. Metals Assimilated by Whole Bacterial Cells Compared to Intracellular Concentrations<sup>a</sup>**

element	whole	interior	whole	interior	whole	interior
	control	control	NAB	NAB	OMT	OMT
Mg ppm	23 600	7720	19 040	4960	6432	5434
%rsd	8	2	2	2	2	2
Al ppm	2360	560	1788	453	9936	703
%rsd	11	5	2	7	0.2	3
P ppm	6800	3580	20 000	5200	28 160	8552
%rsd	7	4	4	4	5	4
Ca ppm	17 200	3400	9600	2267	3360	2248
%rsd	7	4	13	6	10	5
V ppm	5	2	4	2	34	3
%rsd	8	41	52	25	8	13
Fe ppm	2160	354	1364	320	42 880	2662
%rsd	5	4	2	7	5	4
Cu ppm	40	10	60	20	125	51
%rsd	18	12	7	6	5	14
Pb ppm	4	2	3	2	50	3
%rsd	8	3	6	4	3	2
cell dry wt.	whole 10 mg	interior 20 mg	whole 25 mg	interior 29 mg	whole 25 mg	interior 29 mg

<sup>a</sup> ppm =  $\mu\text{g/L} \times \text{mL solution/mg dry cells}$ ; %rsd = percent relative standard deviation.

The greatest cell damage is observed after 24 h when the black particles appear on the interior of the *E. coli* cells, near large voids or vacuoles in the cytoplasm.

## DISCUSSION

Significantly higher concentrations of Al, P, V, Fe, Cu, and Pb are associated with the whole bacteria killed by the OMT leachate (Table 3), than in the live bacteria (controls). In contrast, the concentrations of Mg and Ca are much lower in the OMT leachate-treated whole bacteria. This is consistent with results of Borrok et al.<sup>29</sup> who showed that protons irreversibly exchange with Mg and Ca on the surface of bacteria exposed to acidic solutions and increase adsorption of other metals. Nonetheless, the interior of the OMT treated bacteria shows Mg and Ca concentrations similar to the NAB sample that did not kill *E. coli*, indicating that limitation of these nutrients was not the cause for bacterial cell death.

On the cell interior of the OMT killed bacteria, Al, P, Fe, and Cu have elevated concentrations relative to controls. Whereas Cu can be toxic to bacteria, its abundance is not statistically different than the control or NAB samples. However, concentrations of P, Fe, and Al in the cell interior of OMT killed bacteria are significantly higher than controls.

The high concentration of Al in the OMT leachate is of interest because the antibacterial clay leachates have extreme pH ( $\leq 4$  or  $\geq 10$ ; Table 2). Aluminum is soluble in extreme pH conditions, but precipitates in circum-neutral fluids.<sup>30</sup> Notably, whole-cell concentrations of Al in OMT leachate-treated samples are four times higher than those in the controls, even though the cytoplasmic Al contents in treated and control samples were similar. Apparently, Al has limited transport through cell



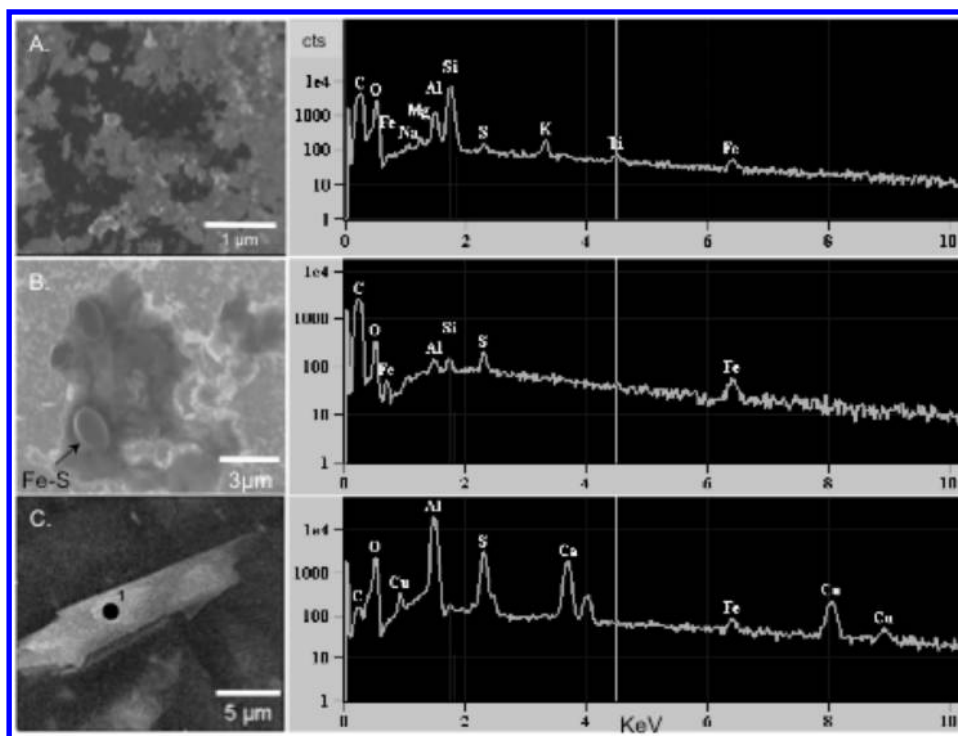


**Figure 2.** SEM images using 30 kV, 2.1 nA current, (A) Clay particles on graphite (dark substrate). EDS (right) shows elements over a rastered area, (B) Close up of Fe–S spherules in aluminosilicate matrix. EDS spectrum is rastered over spherules, (C) Lath shaped particle with high Ca, S, and O (black dot) interpreted as gypsum or jarosite.

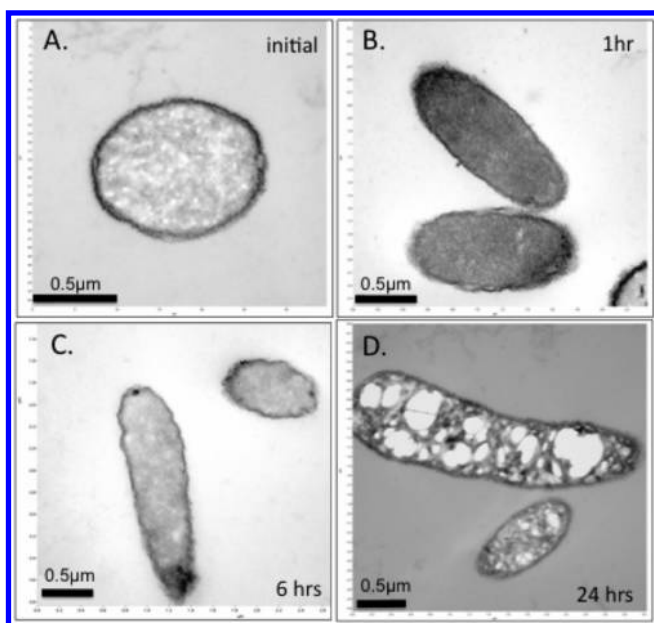


**Figure 3.** Time series TEM images of pressure frozen, fixed (glutaraldehyde and Os vapor), resin embedded, sectioned *E. coli* after incubation with OMT leachate. (A) initial incubation shows uniform black precipitate of electron opaque metal, (B) after 1 h metal migrates toward cell poles, (C) metals are concentrated at cell poles after 6 h, (D) after 24 h metal has penetrated the cell interior and voids form accompanying cell death.

membranes, as tri- and tetra-valent metals are often precluded by cell pore diameters.<sup>31</sup> Aluminum precipitated on the cell envelope might

inhibit influx of nutrients or efflux of waste. However, the elevated intracellular P and Fe suggest that Al did not block their influx channels.

The P content of the *E. coli* killed by OMT leachate is also four times greater than the control, and the interior cell concentration is twice as high. This indicates significant precipitation of P on the cell wall that does not preclude uptake into the cell. Phosphorus is an important part of ATP, DNA, polyphosphates, and phospholipids in cells, and phosphate anions have been found essential for the regulation of cation transport across the cell membrane.<sup>32</sup> The negatively charged phosphate group in the lipid molecules of the cell membrane counterbalance positively charged arginine in a voltage-controlled gate across pore channels. The OMT leachate treated *E. coli* accumulated P, possibly in response to chemical stresses,<sup>33</sup> whereas it was not required in excess for the normal cell function of the controls. The enhancement of P in the *E. coli* cell interior may represent an attempt by the bacteria to control the influx of  $\text{Fe}^{2+}$  across the cell membrane, or to remove the metal.

Whole cell Fe concentrations in the OMT leachate-treated *E. coli* are 20 times greater than in the controls. The intracellular Fe contents are eight times higher. Thus excess Fe was transported through the cell wall and is implicated as the primary reactant in the bactericidal process. The elevated concentrations of P and Fe in the *E. coli* interior imply that extracellular metals did not block transport channels through the cell envelope, at least not initially.

Images depicting the progression of dying *E. coli* incubated with OMT leachate (Figure 3) are similar to images of *E. coli* treated with  $\text{FeSO}_4$ ,<sup>20</sup> where black particles were oxides of  $\text{Fe}^{3+}$ . The vacuoles formed may result from (a) polyphosphate granules that regulate

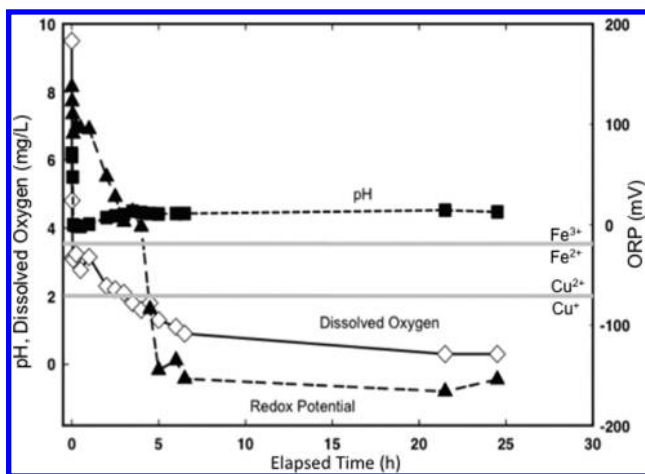


**Figure 4.** Plot showing changes in pH, ORP and dissolved O<sub>2</sub> content of DDI water over 24 h after addition of OMT clay (50 mg/mL). Redox couples for Fe<sup>3+</sup>/Fe<sup>2+</sup> and Cu<sup>2+</sup>/Cu<sup>+</sup> are shown (gray lines) for pH 4.

intracellular metals, (b) metabolic byproducts (e.g., NO), (c) destruction of DNA or other cell components, (d) leakage of cytoplasm after cell death. Bacteria require Fe for many metabolic processes, and use ferritin protein to regulate intracellular Fe levels and storage capacities. Ferritins can keep some Fe in solution, but excess Fe can form toxic precipitates.<sup>34</sup> *E. coli* exposed to OMT leachate may have accumulated P as a stress response<sup>33</sup> and may employ P to gate the cation flux across the cell wall,<sup>32</sup> but eventually the bacteria were overwhelmed by the high Fe<sup>2+</sup> concentration of the OMT leachate.

**Evaluating the Antibacterial Process.** The bioavailability of metals to bacteria depends on the aqueous metal speciation in the clay poultice. The process of transferring elements from a clay surface through water to a cell membrane involves numerous chemical reactions and the formation of rapidly reactive intermediates (radicals) that are affected by clay mineralogy and by surface complexation on the bacteria. The pH and oxidation state of the water added to clay to make a poultice is most influenced by the buffering capacity of the clay minerals with relative surface areas >100 m<sup>2</sup>/g.<sup>35</sup>

Clays that buffer water to circum-neutral pH values are not antibacterial,<sup>6</sup> therefore, we tested the tolerance of *E. coli* to low pH fluids. When the OMT leachates are mixed with *E. coli* growing in LB, the pH increases to 5.3, but this increase does not change the solubility of Fe or Cu (Figure 4). Adjusting the pH of sodium phosphate buffer to acidic conditions similar to that of OMT leachate reduced the population of *E. coli* by 2 orders of magnitude (10<sup>7.5</sup> to 10<sup>5.5</sup> cfu/mL) over 2 h. However, the OMT leachate completely killed the bacteria in less than 1 h,<sup>4</sup> indicating that it is not pH alone that killed the *E. coli*, and implicating soluble species derived from the clay.

The oxidation state of the clay poultice is most critical to the antibacterial process. The highly reduced natural clay buffers the water chemistry of a poultice to low oxidation state where Fe<sup>2+</sup> and Cu<sup>+</sup> are stable (Figure 4). A rapid decrease of dissolved oxygen (D.O.), ORP and pH occurs when the OMT clay is added to DDI water. The pH stabilizes within the first hour, but the D.O. declines over 6 h, coincident with *E. coli* death. It is unlikely that decline in D.O. was responsible for the *E. coli* death, because this bacterium is fully capable of anaerobic respiration.<sup>36</sup> However, *E. coli* may take up Fe<sup>2+</sup> and other metals under anaerobic conditions.

When OMT leachates are oxidized, they lose antibacterial capacity coincident with precipitation of iron oxides. However, if small amounts (50 mg/mL) of clay are suspended in the aqueous solution, the leachate chemistry is stabilized and remains antibacterial. This demonstrates the buffering capacity of the clay.

The OMT clay contains 5–8% pyrite, which is known to be bactericidal. In the presence of water, pyrite produces reactive oxygen species (ROS) such as hydrogen peroxide and hydroxyl radicals that degrade nucleic acids in RNA and DNA via the Fenton reaction.<sup>37</sup> Chelation of Fe<sup>2+</sup> in solution by EDTA, or scavenging of hydroxyl radicals can prevent the destruction of DNA.<sup>38</sup> Therefore, EDTA, thiourea, and bipyridal were used to chelate Fe and remove ROS from OMT aqueous leachates.<sup>4</sup> The bactericidal effect on *E. coli* was reduced (compared to controls), but was not eliminated. Bacteria have developed mechanisms for tolerating external oxidative stress,<sup>39</sup> therefore extracellular ROS are not implicated for bactericide.

Park and Imlay<sup>40</sup> showed that significant damage to cellular DNA occurs when hydrogen peroxide reacts with Fe<sup>2+</sup> to form hydroxyl radicals in vivo. The cell envelope accommodates exogenous hydrogen peroxide,<sup>41</sup> but penetration of Fe<sup>2+</sup> into the cell will catalyze the Fenton reaction. The rapid influx of reduced Fe<sup>2+</sup> and possibly Cu<sup>+</sup> produced by the OMT clay may overwhelm the metal resistance mechanisms of pathogenic bacteria. Oxidation of Fe<sup>2+</sup> occurs *within* the bacteria and there produces destructive hydroxyl radical reactions precipitating Fe<sup>3+</sup> near the intracellular voids (Figure 3d). Hydroxyl radical production may be further enhanced through cellular biochemical reduction of the Fe<sup>3+</sup>.<sup>40</sup> Kohanski et al.<sup>42</sup> showed that production of intracellular hydroxyl radicals is a common underlying mechanism for cellular death by synthetic antibiotics. Evidence suggests that some antibacterial clays promote similar bactericidal reactions.

Development of protective biochemical mechanisms by bacteria<sup>23</sup> may not be possible on the time scale of a clay poultice application. Because of this, the external application of antibacterial clays may be more effective for wound care than systemic antibiotics. The growth of human tissue, coincident with the antibacterial action of clays<sup>1</sup> remains unexplained. However, nanoparticles of Fe-oxide (magnetite) were recently found to be bactericidal against *S. aureus*, while increasing growth of human bone cells.<sup>43</sup> The differential effect of Fe on eukaryotic versus prokaryotic cells is consistent with a role of host defense mechanisms that target bacterial Fe utilization,<sup>44</sup> and may be key to understanding the observed clay healing process.<sup>1</sup>

## AUTHOR INFORMATION

### Corresponding Author

\*Phone: 480-965-0829; fax 480-965-5081; e-mail: Lynda.Williams@asu.edu.

## ACKNOWLEDGMENT

We thank Oregon Mineral Technologies, Inc. for access to their mineral deposit. T. Cunningham and D. Lowry provided TEM images; S. Haydel assisted with microbiology pilot studies. NIH grant R21 AT003618 partially supported this research. We appreciate support from the ASU School of Life Sciences, Center for Solid State Science, and NASA Astrobiology Institute. The author(s) declare that they have no competing interests.

## REFERENCES

- (1) Williams, L. B.; Holland, M.; Eberl, D. D.; Brunet, T.; Brunet de Courssou, L. Killer clays! Natural antibacterial clay minerals. *Mineral. Soc. Bull., London* **2004**, *139*, 3–8.
- (2) Haydel, S. E.; Remenih, C. M.; Williams, L. B. Broad-spectrum in vitro antibacterial activities of clay minerals against antibiotic—susceptible and antibiotic-resistant bacterial pathogens. *J. Antimicrob. Chemother.* **2008**, *61*, 353–361.
- (3) Williams, L. B.; Haydel, S. E.; Geise, R. F.; Eberl, D. D. Chemical and mineralogical characteristics of French green clays used for healing. *Clays Clay Miner.* **2008**, *56*, 437–452.
- (4) Cunningham, T. B.; Koehl, J. L.; Summers, J. S.; Haydel, S. E. pH-dependent metal ion toxicity influences of the antibacterial activity of two natural mineral mixtures. *PLoS-ONE*. **2010**, *5*, e9456.
- (5) Ferris, F. G.; Fyfe, W. S.; Beveridge, T. J. Bacteria as nucleation sites for authigenic minerals in a metal-contaminated lake sediment. *Chem. Geol.* **1987**, *63*, 225–232.
- (6) Williams, L. B.; Haydel, S. E. Evaluation of the medicinal use of clay minerals as antibacterial agents. *Int. Geol. Rev.* **2010**, *52*, 745–770.
- (7) Metge, D. W.; Harvey, R. W.; Eberl, D. D.; Wasylenki, L. E.; Williams, L. B. Evaluating the oxidation state of antibacterial minerals. *Geochim. Cosmochim. Acta, Suppl.* **2009**, *73*, A875.
- (8) Clark, C. J.; McBride, M. B. Chemisorption of  $\text{Cu}^{2+}$  and  $\text{Co}^{2+}$  on allophane and imogolite. *Clays Clay Miner* **1984**, *32*, 300–310.
- (9) Onodera, Y.; Sunayama, S.; Chatterjee, A.; Iwasaki, T.; Satoh, T.; Suzuki, T.; Mimura, H. Bactericidal allophonic materials prepared from allophane soil II. Bactericidal activities of silver/phosphorus-silver loaded allophonic specimens. *Appl. Clay Sci.* **2001**, *18*, 135–144.
- (10) Magaña, S. M.; Quintana, P.; Aguilar, D. H.; Toledo, J. A.; Angeles-Chavez, C.; Cortez, M. A.; Leon, L.; Freile-Peleorio, Y.; Lopez, T.; Torrex-Sanches, R. M. Antibacterial activity of montmorillonites modified with silver. *J. Mol. Catal.* **2007**, *A281*, 192–199.
- (11) Sawai, J.; Yoshikawa, T. Quantitative evaluation of antifungal activity of metallic oxide powder (MgO, CaO and ZnO) by an indirect conductimetric assay. *J. Appl. Microbiol.* **2004**, *96*, 803–809.
- (12) Waltimo, T.; Brunner, T. J.; Vollenweider, M.; Stark, W. J.; Zehnder, M. Antibacterial effect of nanometric bioactive glass. *J. Dent. Res.* **2007**, *86*, 754–757.
- (13) Yacoby, I.; Benhar, I. Antibacterial Nanomedicine. *Nanomedicine* **2008**, *3*, 329–341.
- (14) Jackson, M. L. *Soil Chemical Analysis Advanced Course*, 2nd ed.; Madison, WI, 1979.
- (15) Tovar-Sanchez, A.; Sanudo-Wilhelmy, S. A.; Garcia-Vargas, M.; Weaver, R. S.; Popels, L. C.; Hutchins, D. A. A trace metal clean reagent to remove surface-bound iron from marine phytoplankton. *Mar. Chem.* **2003**, *82*, 91–99.
- (16) Vogel, C.; Fisher, N. S. Metal accumulation by heterotrophic marine bacterioplankton. *Limnol. Oceanogr.* **2010**, *55*, 519–528.
- (17) Eberl, D. D. *Users guide to RockJock: A Program for Determining Quantitative Mineralogy from Powder X-ray Diffraction Data*, Open file Report 03-78; U. S Geological Survey: Denver, CO, 2003.
- (18) Cohn, C.; Laffers, R.; Simon, S. R.; O’Riordan, T.; Schoonen, M. A. A. Role of pyrite in formation of hydroxyl radicals in coal: possible implications for human health. *Part. Fibre Toxicol.* **2006**, *3*.
- (19) Source Clays Repository, Clay Minerals Society Website; <http://www.clays.org> (accessed February 27, 2011).
- (20) Lee, C.; Kim, J. Y.; Lee, Y.; Nelson, K. L.; Yoon, J.; Sedlak, D. L. Bactericidal effect of zero-valent iron nanoparticles on *Escherichia coli*. *Environ. Sci. Technol.* **2008**, *42*, 4927–4933.
- (21) Hauser, E. A. Kisameet Bay clay deposit. In *Problems of Clay and Laterite Genesis*; American Institute of Mining and Metallurgical Engineering: New York, 1952; pp 178–190.
- (22) Dopson, M.; Baker-Austin, C.; Koppineedi, P. R.; Bond, P. L. Growth in sulfidic mineral environments: metal resistance mechanisms in acidophilic microorganisms. *Microbiology* **2003**, *1490*, 1959–1970.
- (23) Nies, D. H. Microbial heavy-metal resistance. *Appl. Microbiol. Biotechnol.* **1999**, *51*, 730–750.
- (24) Wackett, L. P.; Dodge, A. G.; Ellis, L. B. Microbial genomics and the periodic table. *Appl. Environ. Microbiol.* **2004**, *70*, 647–655.
- (25) Gikunju, C. M.; Lev, S. M.; Birenzvege, A.; Schaefer, D. M. Detection and identification of bacteria using direct injection inductively coupled plasma mass spectroscopy. *Talanta* **2004**, *62*, 741–744.
- (26) Helgeson, H. C. Thermodynamics of hydrothermal systems at elevated temperatures and pressures. *Am. J. Sci.* **1969**, *267*, 729–804.
- (27) Beveridge, T. J. Structures of Gram-negative cell walls and their derived membrane vesicles. *J. Bacteriol.* **1999**, *181*, 4725–4733.
- (28) Shapiro, L.; McAdams, H.; Losick, R. Generating and exploiting polarity in bacteria. *Science* **2002**, *298*, 1942–1946.
- (29) Borrok, D.; Fein, J. B.; Tischler, M.; O’Loughlin, E.; Meyer, H.; Liss, M.; Kemner, K. M. The effect of acidic solutions and growth conditions on the adsorptive properties of bacterial surfaces. *Chem. Geol.* **2004**, *209*, 107–119.
- (30) Wesolowski, D. J. Aluminum speciation and equilibria in aqueous solution: I. The solubility of gibbsite in the system Na-K-Cl-OH-Al-Al(OH)<sub>4</sub> from 0 to 100°C. *Geochim. Cosmochim. Acta* **1992**, *56*, 1065–1091.
- (31) Williams, R. J. P. What is wrong with aluminum?]> *J. Inorg. Biochem.* **1999**, *76*, 81–88.
- (32) Schmidt, D.; Jiang, Q.; MacKinnon, R. Phospholipids and the origin of cationic gating charges in voltage sensors. *Nature* **2006**, *444*, 776–779.
- (33) Rao, N. N.; Liu, S.; Kornberg, A. Inorganic polyphosphate in *Escherichia coli*: the phosphate regulon and the stringent response. *J. Bacteriol.* **1998**, *180*, 2186–2193.
- (34) Arosio, P.; Levi, S. Ferritin, iron homeostasis and oxidative damage. *Free Radical Biol. Med.* **2002**, *33*, 457–463.
- (35) Moore, D. M.; Reynolds, R. C. *X-ray Diffraction and the Identification and Analysis of Clay Minerals*; Oxford University Press: New York, 1997.
- (36) Unden, G.; Achebach, S.; Holighaus, G.; Tran, H.; Wachwitz, B.; Zeuner, Y. Control of FNR function of *Escherichia coli* by O<sub>2</sub> and reducing conditions. *J. Mol. Microbiol. Biotechnol.* **2002**, *4*, 263–268.
- (37) Schoonen, M. A. A.; Harrington, A. D.; Laffers, R.; Strongin, D. R. Role of hydrogen peroxide and hydroxyl radical in pyrite oxidation by molecular oxygen. *Geochim. Cosmochim. Acta* **2010**, *74*, 4971–4987.
- (38) Cohn, C. A.; Fisher, S. C.; Brownawell, B. J.; Schoonen, M. A. A. Adenine oxidation by pyrite generated hydroxyl radicals. *Geochem. Trans.* **2010**, *11* (2), 8.
- (39) Storz, G.; Tartaglia, L. A.; Farr, S. B.; Ames, B. N. Bacterial defenses against oxidative stress. *Trends Genet.* **1990**, *6*, 363–368.
- (40) Park, S.; Imlay, J. A. High levels of intracellular cysteine promote oxidative DNA damage by driving the Fenton reaction. *J. Bacteriol.* **2003**, *185*, 1942–1950.
- (41) Imlay, J. A.; Linn, S. Toxic DNA damage by hydrogen peroxide through the Fenton reaction in vivo and in vitro. *Science* **1988**, *240*, 640–642.
- (42) Kohanski, M. A.; Dwyer, D. J.; Hayete, B.; Lawrence, C. A.; Collins, J. J. A common mechanism of cellular death induced by bactericidal antibiotics. *Cell*. **2007**, *130*, 797–810.
- (43) Tran, N.; Mir, A.; Mallik, D.; Sinha, A.; Nayar, S.; Webster, T. J. Bactericidal effect of iron oxide nanoparticles on *Staphylococcus aureus*. *Int. J. Nanomed.* **2010**, *5*, 277–283.
- (44) Repine, J. E.; Fox, R. B.; Berger, E. M. Hydrogen peroxide kills *Staphylococcus aureus* by reacting with Staphylococcol iron to form hydroxyl radical. *J. Biol. Chem.* **1981**, *256*, 7094–7096.